

DYNAMIC INVESTIGATION OF TWIST-BEND COUPLING IN A WIND TURBINE BLADE

MARCIN LUCZAK

Institute of Fluid-Flow Machinery Polish Academy of Sciences, Gdańsk, Poland
e-mail: marcin.luczak@imp.gda.pl

SIMONE MANZATO, BART PEETERS

LMS International, Leuven, Belgium
e-mail: simone.manzato@lmsintl.com

KIM BRANNER, PETER BERRING

Wind Energy Division, Risø DTU, Denmark
e-mail: kibr@risoe.dtu.dk

MACIEJ KAHSIN

Gdansk University of Technology, Gdańsk, Poland
e-mail: mkahsin@pg.gda.pl

This paper presents some results and aspects of the multidisciplinary and interdisciplinary research oriented for the experimental and numerical study in static and dynamic domains on the bend-twist coupling in the full scale section of a wind turbine blade structure. The main goal of the conducted research is to confirm experimentally the numerical prediction of modification of the dynamic and static properties of a wind turbine blade. The bend-twist coupling was implemented by adding angled UD (UniDirectional) layers on the suction and pressure side of the blade. Static and dynamic tests were performed on a section of the full scale wind turbine blade provided by Vestas Wind Systems A/S. The results are presented and compared with the measurements of the original and modified blade. Comparison analysis confirmed that UD layers introduce measurable bend-twist couplings, which was not present in the original blade.

Key words: wind turbine blade, bending, torsion, composite materials

1. Introduction

Wind turbine blades must be designed to resist the extreme load cases and fatigue loads from normal operation. Sudden wind gusts are often too quick for the active pitch control system to react and may shorten the fati-

gue life substantially. This problem may be overcome by an aero-elastic tailoring of the blades. Particular implementation of an anisotropic composite material can introduce bend-twist coupling in the blade (Deilmann, 2009; Lobitz and Laino, 1998; Lobitz and Veers, 1999; Lobitz *et al.*, 2001; Locke and Valencia, 2004; Ong and Tsai, 1999; Walsh, 2009; Zuteck, 2002). The coupling causes the feathering blade to twist under the bending load, and as a result decreases the angle of attack. This paper presents the progress and results of a comprehensive long-term scientific research focused on bend-twist coupling analysis, design and implementation in a wind turbine blade made from composite materials. First three parts of the paper briefly recall the research activity carried out (Berring *et al.*, 2007; Branner *et al.*, 2007; Fedorov *et al.*, 2010) while the main focus is put on the measuring and modeling of the dynamic behavior described within the fourth part.

The first part of the paper reports on the experimental and numerical studies of a standard wind turbine blade section. The wind turbine blade section made of a composite material was statically tested and modeled. Different load configurations were applied at the tip of the blade section to assess the twist and bend behavior (Berring *et al.*, 2007).

The second part of the paper presents the structural dynamics identification, which was performed by means of experimental modal analysis. The Finite Element Method model (FEM) (Branner *et al.*, 2007) was developed, updated and validated against the static measurement results. A part of this work has been published in Luczak *et al.* (2011). Based on the validated model the modified design of existing blade was studied. The baseline concept of the modification was implementation for bend-twist coupling by means of application of additional composite material layers. The original blade section was modified with four layers of UD1200 (glass fibre, 1200 g/m²), which were laminated on the pressure and suction side of the blade, with an angle of 25 degrees to the blade axis, in order to create a measurable flapwise bend-twist coupling.

In the third part, the static experimental and numerical analysis of the modified blade section is exposed to verify the design correctness of the bend-twist coupling.

Finally, in the fourth part the dynamic behavior of the modified blade section is experimentally identified with the assessment of the coupling. Moreover, the influence of the support structure dynamics on the test specimen is discussed.

2. Static investigation of original blade section

Static loads in bending, torsion and combined bending and torsion configurations were introduced with different loading force levels (Berring *et al.*, 2007; Branner *et al.*, 2007; Fedorov *et al.*, 2010).

2.1. Object of the investigations

The object of investigation is an 8 meter long section cut from a 23 meter wind turbine blade. This section is mounted in two root clamps with an additional clamp at the tip for hydraulic jack fastening (Fig. 1).

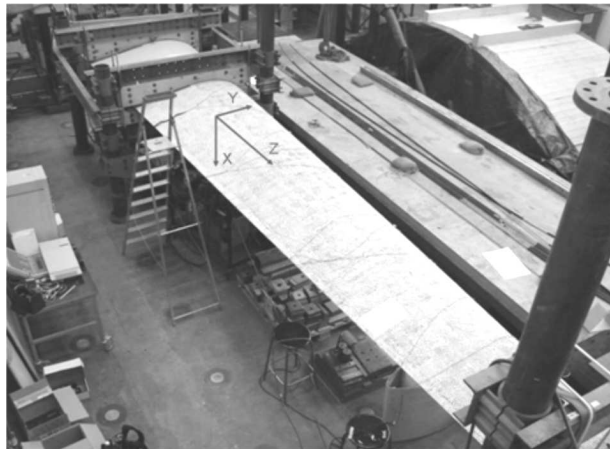


Fig. 1. Wind turbine blade section under investigation with the coordinate system.
For measurements of the original blade, the axis system is rotated of 90°
about z axis

Bending angles are computed considering the rotation of two consecutive measured cross-sections about the x axis. The twist angles are computed as the rotation about the z axis of each cross section with respect to the unloaded configuration. A detailed description of the calculation can be found in Berring *et al.* (2007). Figure 2 shows the bend and twist angles of the original blade computed from the static bending measurement.

The graph indicates that the bend-twist coupling is equal or close to zero, since the bending moment does not result in a twist angle (rotation about the z axis) of the blade section.

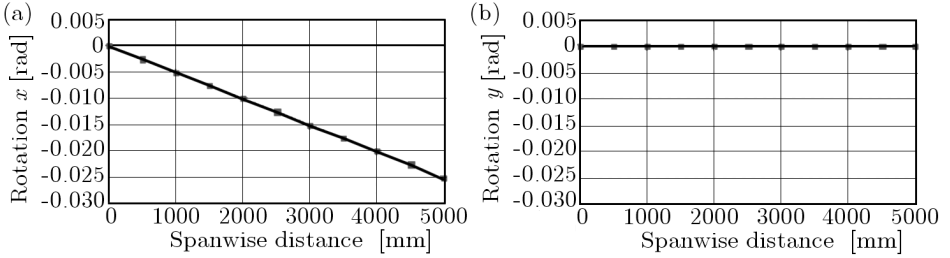


Fig. 2. Bending slope angle (a) and cross-sections twist angle (b) values under flapwise bending load. The blade section is bending but not twisting. That indicates that the bend-twist coupling is close to zero

3. Dynamic investigation of the original blade section

Observations from the static investigations were verified in the structural dynamics of the tested original blade section (Capellaro, 2006). Measurement points were defined on the leading and trailing edge at thirteen cross-sections. Flapwise and edgewise direction accelerations were measured. Points on the support structure were not measured. As the drawback of this fact, some of the natural frequencies of the support structure were indentified as the modes of the blade while they are modes of the support structure. Natural frequencies and corresponding mode shapes were estimated and some examples are presented in Fig. 3.

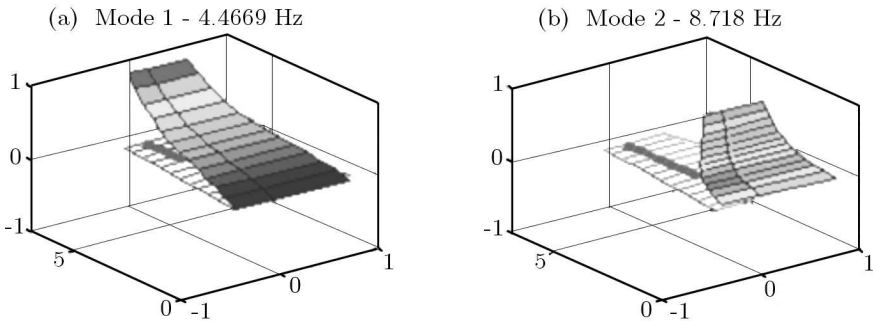


Fig. 3. 3D plots of mode shapes of the original blade section. First flap wise bending (a) and first edgewise bending (b)

4. Static investigation of the modified blade section

One of the primary aims of this long-term research is to study, design and implement the desired bend-twist coupled behavior. The original blade section was modified with four layers of UD1200, which were laminated on the pressure and suction side of the blade with the fibers angle of 25° to create a measurable flapwise bend-twist coupling. The additional layers were laminated as indicated in Fig. 4.

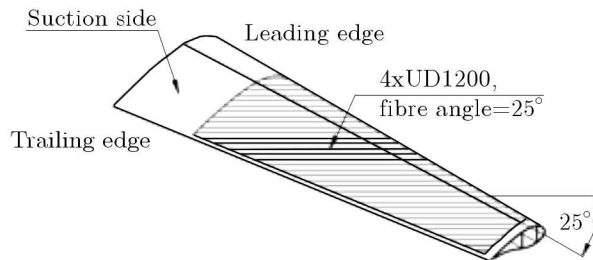


Fig. 4. Fiber orientations of the extra UD layers

To verify the numerical prediction of the bend-twist coupling, the static tests campaign from the original blade was repeated on the modified blade. The twist angles for equidistant cross-sections under flapwise bending load were calculated from the measurement (Fig. 5).

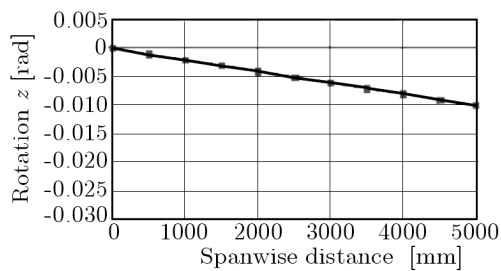


Fig. 5. Twist angle under flapwise bending load. This indicates that the blade section has a measurable bend-twist coupling

Assuming that the shear center is located in the center of the spar, the rotation angles about the z axis for the modified blade section in Fig. 5 show a measurable bend-twist coupling.

5. Dynamic investigation of modified blade section

The flapwise bend-twist coupling was also investigated by means of experimental modal analysis. The research was focused on the bend-twist coupling presence in the mode shapes of the blade section. An important aspect was also the analysis of the influence of an additional mass and stiffness introduced by the extra layers. Finally, the influence of the support structure on the correlation analysis between the numerical and the experimental modal models was studied (Luczak *et al.*, 2010; Peeters *et al.*, 2004).

The blade section was excited by two electro-dynamic shakers attached at the tip end in the flapwise and the edgewise directions. Frequency Response Functions were measured and stored within 0 and 120 Hz frequency range.

For adequate identification of the blade dynamic displacement, accelerations of the vibrations were measured in 130 points. Thirteen equidistant measurement cross-sections were defined along the span wise direction (Z) every 0.5 m. Each cross section contains five measurement points in which the accelerations were acquired along the flapwise (X) and edgewise (Y) directions. These points were located at the leading edge, trailing edge, on the line of the airfoil maximum thickness and in the mid-points between the previous three. The measurement directions were precisely defined based on the CAD (Computer Aided Design) geometry of the blade section.

The model quality assessment was an integrated part of the investigation. The following conditions have to be fulfilled to satisfy the modal analysis assumptions: time invariance linearity, Maxwell's reciprocity principle and observability. Possible sources of nonlinearities within the investigated structure are material properties, geometrical properties and the existence of bond connections. Verification of the superposition rule is one of the methods of detecting nonlinearities. Linearity check was performed for several levels of driving voltage ranging from 0.5 V to 2 V with a step of 0.5 V. The results are presented in Fig. 6. The Frequency Response Function (FRF) between the input signal and the output spectrum defined as the acceleration over force, remains constant independently of the excitation voltage level. This proves that the structure dynamic behavior is linear within the bandwidth of interest.

The reciprocity check is based on Maxwell's principle, which states that the FRFs obtained by applying the force in point 1 and measuring the response in 2 and *vice versa* should be the same. The results for the two checks performed confirmed applicability of the reciprocity rule.

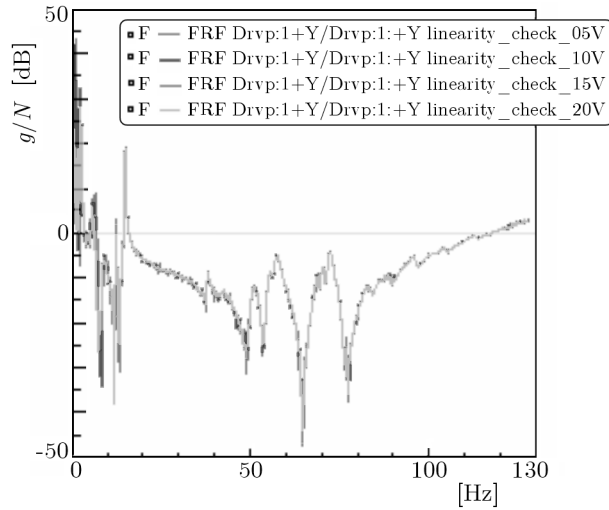


Fig. 6. Linearity check for one of the points on the blade. Voltage values = 0.5 V, 1 V, 1.5 V and 2 V

During the processing of data some significant noise was observed in the acquired FRFs in the low frequency region. The driving points coherence functions show a small drop in this region, meaning a non-ideal excitation (Fig. 7).

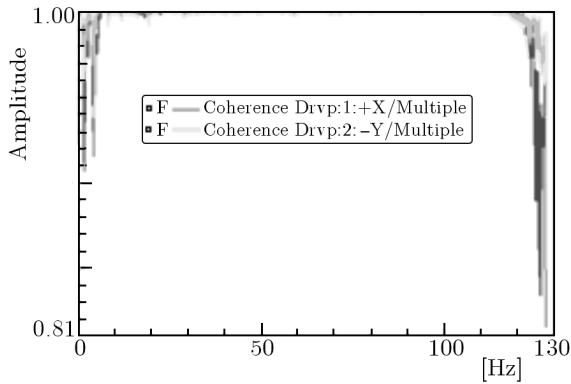


Fig. 7. Coherence functions for the two driving points. Measure of the FRF quality is used. Ideally, it should take value equal to 1

The modal parameter identification technique was not able to clearly stabilize the modes in this region, possibly resulting in some local errors in the mode shapes below 7 Hz. The estimation provided natural frequencies, mode shapes and corresponding damping ratios in the frequency bandwidth 0-60 Hz. The first five out of 12 identified mode shapes are shown in Fig. 8.

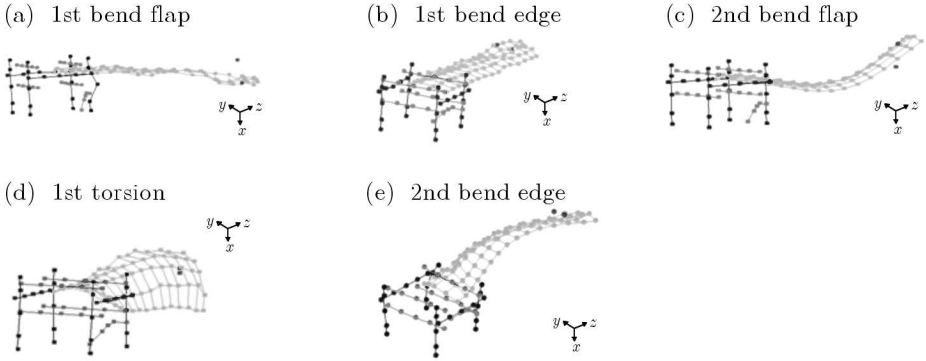


Fig. 8. Estimated experimental mode shapes of the modified blade section and support structure

The MAC (Modal Assurance Criterion) can be used to compare two modal models. The MAC between two mode shape vectors, ϕ_i and $\phi_i(s)$, is defined as

$$\text{MAC}(s) = \frac{|\phi_i^\top \phi_i(s)|^2}{\phi_i^\top \phi_i \phi_i^\top(s) \phi_i(s)} \quad (5.1)$$

If a linear relationship exists between the two complex vectors ϕ_i and $\phi_i(s)$, the MAC value will be near to 100. If they are linearly independent, the MAC value will be small (near zero). Figure 9 shows a comparison between the AutoMAC of the modal model obtained by considering only the sensors on the blade and the one where also the sensors on the supporting structure were included.

Low valued off-diagonal terms for the blade without the support structure model ensure linear independence of the estimated modal vectors. The correlation between off-diagonal terms is increased when including the supporting structure in the analysis. This is due to the fact that the clamping is not perfectly rigid and the support has its own dynamic behavior which influences the measured response of the blade.

In Fig. 9, the red color corresponds to the MAC value equal to 100. The dark blue color reflects the MAC value 0. The modes corresponding to frequencies 8 Hz, 28 Hz, 31 Hz and 33 Hz are related to dynamic properties of the supporting structure.

5.1. Correlation analysis for the simulation and test results

Using the modal model estimated experimentally and those obtained from the FEM models (modeling the original and modified blades), the correlation

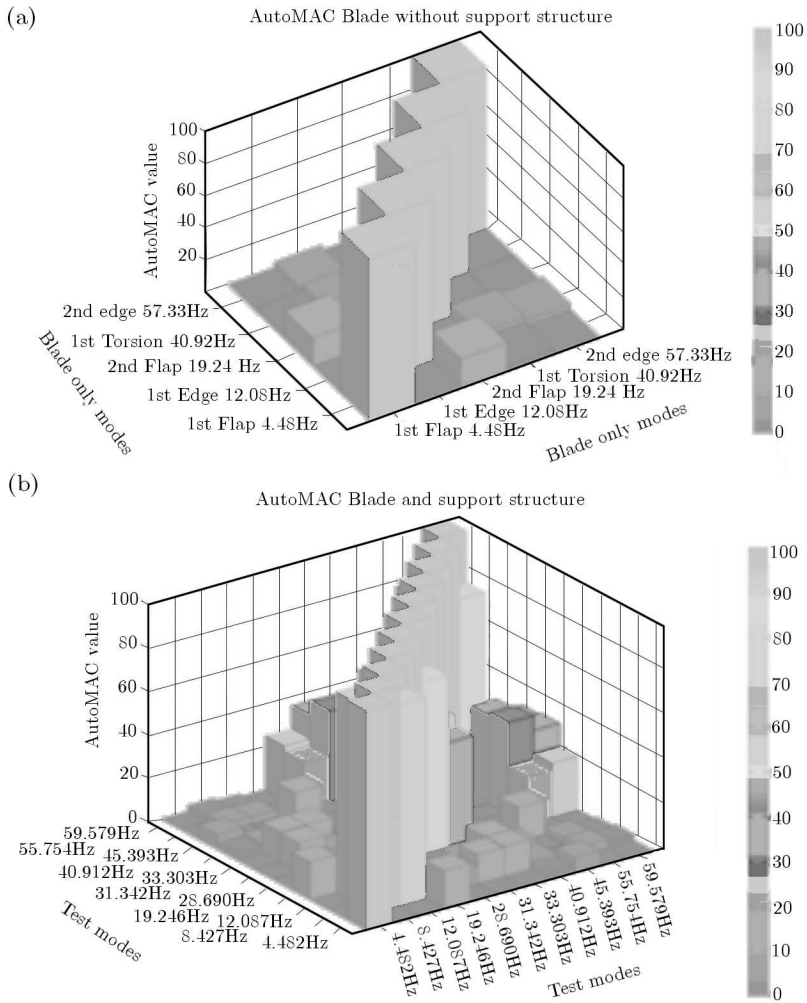


Fig. 9. AutoMAC matrices for the experimental modal model with sensors only on the modified blade section (a) and blade section with the support structure (b)

analysis can be applied. The FEM models should be characterized by good consistency of the natural frequency values and mode shapes obtained from the measurement. The Modal Assurance Criterion is used as the original-modified blade simulation and also test-simulation correlation metrics.

The global axis system used to define the test model differs from that used in the FEM model. In order to match the models, it is necessary to apply geometric correlation by translation and rotation of the test model (Fig. 10). The next step is node mapping. The number of measurement nodes is much

smaller than the FEM nodes. Modal vectors are compared only for the nodes from FEM which are located closest to the measurement points. Only the portion of the blade past the clamp is considered.

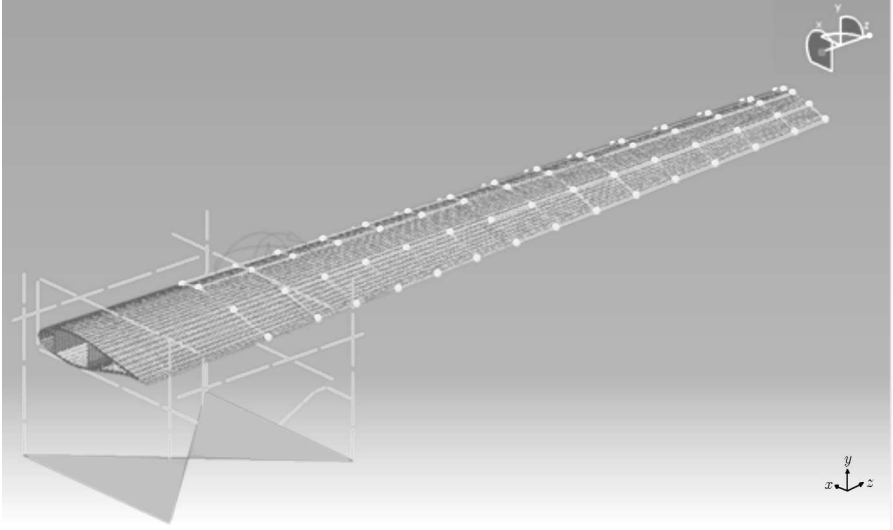


Fig. 10. Test and FEM geometry correlation with node mapping

For tests described in section 2 to 4, the support structure was not taken into account and measured data reduced to obtain a perfectly rigid boundary condition on the clamped section (Berring *et al.*, 2007; Branner *et al.*, 2007; Fedorov *et al.*, 2010; Larsen *et al.*, 2002; Pedersen and Kristensen, 2003). Since the FEM model of the blade is developed using the same assumption, some differences in the frequency values and mode shapes obtained from experimental results of the modified blade are expected.

The blade model was used to compute mode shapes in the 0-60 Hz frequency bandwidth and computations were performed on a $50T_{flop}$ (10^{12} FLoating point OPerations per second) cluster in TASK Super Computing Center.

The first Modal Assurance Criteria were calculated for the corresponding modes in order to associate the closest numerical and experimental mode shapes (Fig. 11). The procedure accounted for both natural frequency value and the mode shape consistency.

The following modes were investigated: 1st and 2nd flapwise bending, 1st and 2nd edgewise bending and 1st torsional (Fig. 8). The MAC matrix in Fig. 11 clearly shows that the off-diagonal terms are low valued, which confirms the linear independence of estimated modal vectors. The best test and simulation modal vectors consistency can be observed for the 2nd flapwise mo-

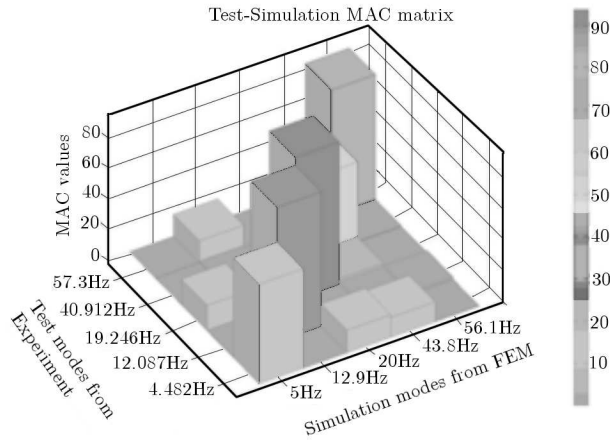


Fig. 11. MAC matrix for test and FEM simulation modal vectors of the modified blade without the support structure

de. The consistency of the results can be recognized as satisfactory, however the present differences should be further investigated. Observing the values of the MAC criterion between the test and simulation modes (Fig. 9), some differences can be observed. They are caused by the influence of the support structure and not perfectly excited the 1st bending mode.

Comparison of the natural frequencies obtained from experimental measurements and simulation for the original and modified blade is presented in Table 1.

Table 1. Comparison of the natural frequencies for the experimental and numerical results obtained for the original and modified blade

Original blade FEM	Original blade Test	Modified blade FEM	Modified blade Test
1st bend flap			
4.7 Hz	4.5 Hz	5.01 Hz	4.48 Hz
1st bend edge			
10.85 Hz	8.7 Hz	12.9 Hz	12.08 Hz
2nd bend flap			
18.56 Hz	18.9 Hz	20.03 Hz	19.24 Hz
1st torsion			
42.99 Hz	39.5 Hz	43.75 Hz	40.92 Hz

The difference between the Test and FEM frequencies can be explained by modeling the boundary condition as rigid in the FEM. Moreover, further differences in the frequency values between the original and modified blade results are introduced by the additional mass and stiffness implemented from angled UD layers on the suction and pressure side of the blade. These UD layers introduce measurable bend-twist couplings, not present in the original blade in terms of static and dynamic response of the investigated section of the blade. While in the static response there was a clear indication of the coupling, the modification of the dynamic stiffness is not fully recognized, which can be observed based on the comparison of the simulation of original and modified blade structural dynamics (Fig. 12).

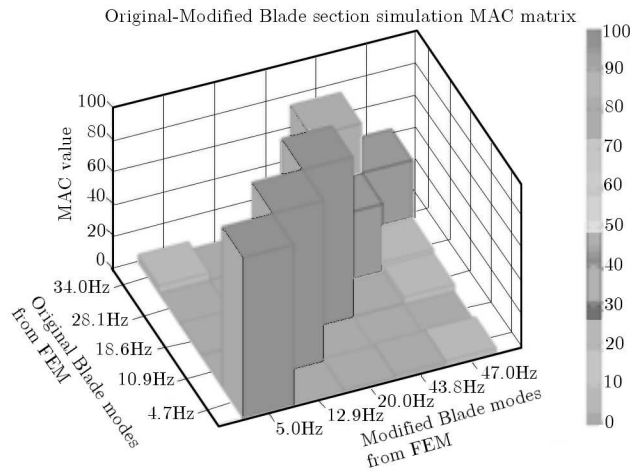


Fig. 12. MAC matrix for the original and modified blade Finite Element models

100% MAC matrix terms for the first three modes may indicate that these particular mode shape sensitivity towards the implemented additional layers is not significant.

5.1.1. FEM model of the blade section with FEM model of the support structure

The numerical model adopts the previously developed MSC.Patran/Nastran blade FEM model comprised of 8-node shell elements (Quad8) and the 20-node solid elements (Hex20). This model has approximately 600.000 degrees of freedom (Berring *et al.*, 2007). The original FEM model of the blade was developed to study the static response, i.e. cross sectional displacements and rotations caused by different load configurations. A least squares algorithm was developed, which fits a plane through each deformed cross section, and

defines a single set of displacements and rotations (three displacements and rotations) per cross section. This least squares algorithm was also used to accommodate problems with a flexible boundary condition by determining the displacements and rotations for a cross section near the boundary. These displacements and rotations are subtracted from all other cross-sections along the blade and thereby making the blade section fully fixed at the chosen cross section near the boundary (Fig. 13).

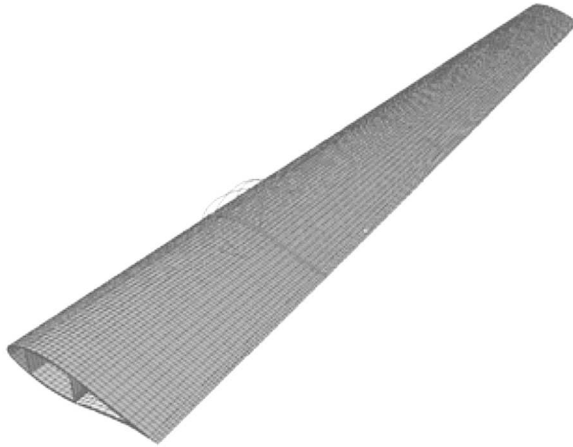


Fig. 13. Original FEM model of the blade

The boundary conditions which were adequately representing the support structure in static analysis were used in the initial theoretical modal analysis. In the correlation analysis of the test and FEM modal models, it turned out that a non-negligible discrepancy in mode shapes occurs. A relatively light and flexible support (Fig. 14a) has significant contribution to the simulated mode shapes of the studied structure which can be observed in the MAC values (Fig. 11). It was assumed that introducing into the FEM model the representation of the supporting structure could improve the test-simulation results correlation.

The uncertainties concerning the support structure makes the modeling process rather challenging. As the source of uncertainties one can point not only geometrical and material parameters of the support members, but mainly their connections. Additionally, analyzing the test modal model it can be seen that these connections are very flexible, therefore very important in the overall dynamical behavior of the analyzed system. As the future activity optimization based updating has been foreseen. The fine-tuning of the FEM model is iterative, therefore, due to the size of the simulated model the main

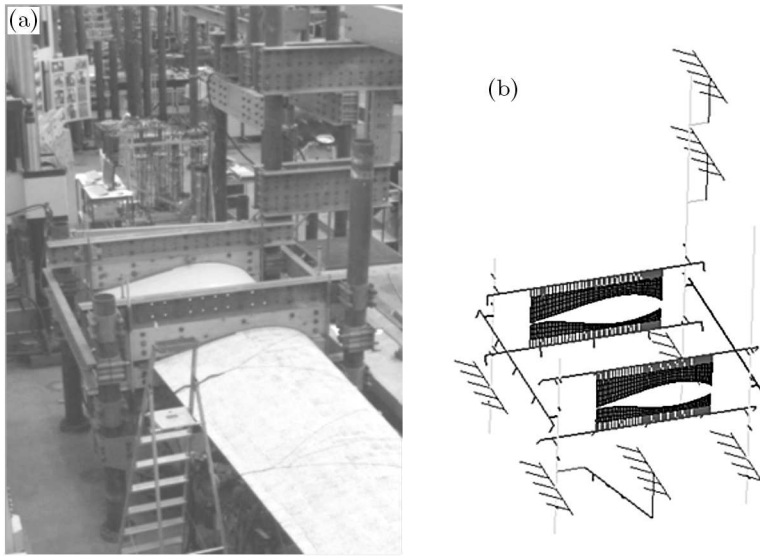


Fig. 14. Supporting structure (a) and its FEM model (b)

assumption prior modification of the original FEM model (blade only model) was to keep the additional FEM model (i.e. supporting structure) as simple as possible. The derived model allows correlating the simulation results with measured data in all points used in the tests.

As it can be seen in Fig. 14a, the real supporting structure comprises of pipes, UNP-profiles (according to European Standard tables for steel profiles), and support clamps of contour-cut plywood. Basic information about the geometry and material properties exploited in the derived additional FEM model are presented in Table 2.

Table 2. Basic information about geometry and material properties used for modeling of the supporting structure

	Pipes	C-Shapes	I-Shapes	Plywood
Geometry [mm]	Inner radius 170 Outer radius 160	Standard UPN 200	Two bolted standard UPN 200	Thickness 180
E modulus [GPa]	200	200	200	13.2
Density [kg/m ³]	7890	7890	7890	736
Poisson's ratio	0.3	0.3	0.3	0.01

In the modified FEM model, the steel members (i.e. pipes and UNP profiles) are modeled by beam elements (CBEAM in Nastran notation). The plywood in clamps is modeled by shell elements (CQUAD4). All mountings between the support members are represented by elastic spring elements (CELAS1). It should be noted that beam elements representing the frame are placed at the centerline of the frame members. As a consequence, discrepancy between the nodes of the FEM model and geometrical positions of measuring points exists. For the correlation, additional nodes were inserted at the measuring points. Connections between the beams and the additional nodes were realized by the use of rigid bar elements (RBAR). Due to the same fact, there were gaps between the beams and plywood in the FEM model representation of the clamps (Fig. 12). Nodes of the beams and shells elements constituting the clamp were connected by the use of rigid bar elements (RBE2). The rigid connection between the plywood and I shapes is justified because of the large difference in E modules of both materials. Representation of FE-to-test matching with the rigid bars does not introduce additional stiffness to the system and is acceptable as long as the global mode shapes of the support are of interest only. After preparation of the support FE model, both the additional and the original FE models were merged (Fig. 15). The nodes at the interface

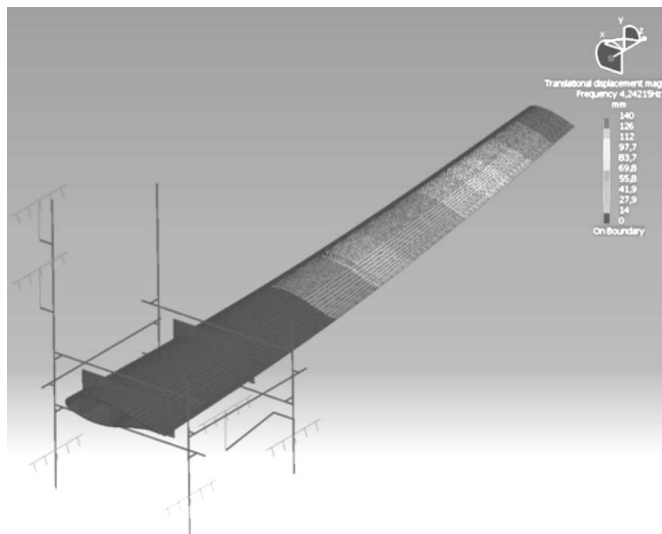


Fig. 15. Updated FEM model of the blade with the flexible supporting structure

between the blade and supporting structure, i.e. between the plywood and the outer surface of the blade, have restrained rotational DOFs (Degree Of Freedom). Such an approach was taken because in the real structure the interface

between the profile-cut plywood and the blade is realized on approximately 200 mm of width, while in the numerical model a single row of nodes is used only.

An initial correlation analysis of updated FEM model is presented in Fig. 16.

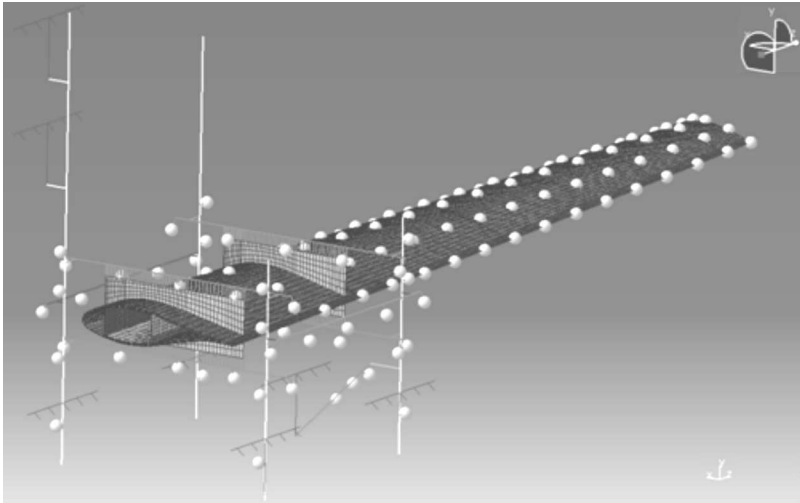


Fig. 16. Geometry correlation of the TEST and FEM models of the modified blade section with the support structure. 124 out of 132 measurement points are now coupled with the FEM nodes

The initial correlation results of the updated FEM model show an improvement in comparison with the results from the original FEM model (Fig. 17).

5.2. Computation of twist and bend angles

Using the modal vectors identified from the experimental modal analysis results or computed from the FEM model, the twisting and bending angles for particular mode shapes can be computed. For the experimental mode shapes, a fitting is applied to smooth out some odd local behavior due to inherent errors in the measuring process and excitation limitations shown in Fig. 7.

For the twisting angles, a similar approach to the one used in the static computation is applied (Berring *et al.*, 2007). For each cross-section, displacements from the undeformed configuration are associated with the estimated modal amplitudes. Only the leading and trailing edge results are used in the computation. Both relative angles for each section and the sum of these angles along the blade were computed.

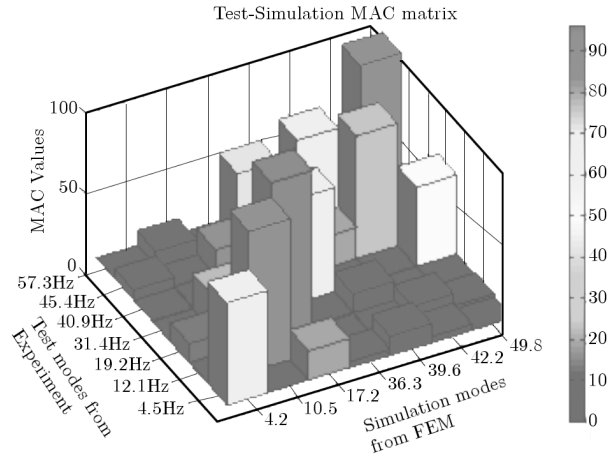


Fig. 17. MAC matrix, Test vs. updated FEM model of the blade with the flexible support

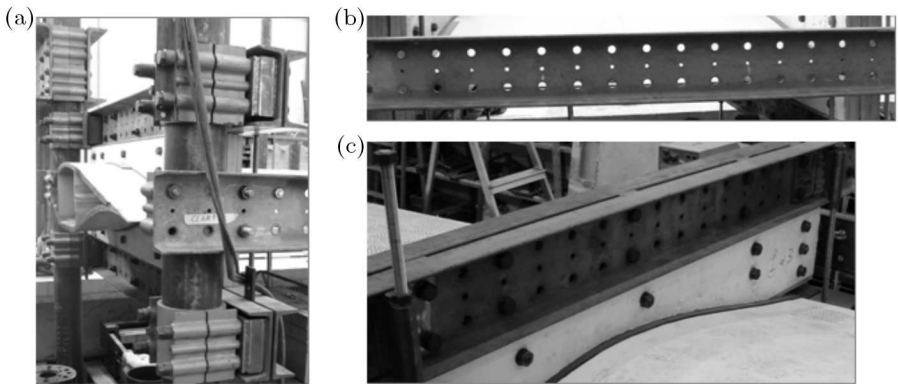


Fig. 18. Mountings of the supporting structure (a), drilled UPN (b), two bolted UPN (c)

Bending angles were computed in a slightly different way than for static measurements. The modal displacements obtained from the sensors located in the point of the maximum thickness of the airfoil for each section are considered. By considering two consecutive cross-sections, relative bending is evaluated as the difference between the modal displacements in the x direction (see Fig. 1). The tangent of the relative angle for the section is then computed by dividing the difference for the length of the section. On each cross-section, the global bending angle is computed by summing all the relative angles for the previous cross-sections. Computed angles are modal angles, so they depend

on the scaling applied to the modal vectors. Moreover, torsional angles are computed assuming that the mass and shear centers are in the same locations.

5.3. Numerical and experimental twist and bend angles

The methodology described in Section 5.2 is applied both to numerical and experimental modal analysis results. In the present paper, only a limited part of the experimental results is presented in details. The results for the first and second flap modes will be discussed. The original blade simulation flap bending translation values (Fig. 19a,e) are plotted with the dark blue, edge bending with red and rotation with light blue. The original blade experimental results are presented in Fig. 19c,g. Deflection in the flap direction is plotted with the red line, edgewise direction with blue and rotation around the blade axis is marked with green. The angles values are assumed to be 0 in the clamped section.

For the modified blade section bending angle, the values are plotted in dark blue and twist in red. In order to have an overview of the overall behavior, the absolute angles are presented. The results are obtained by processing the fitted mode shapes.

By graphically comparing the original and modified blade plots (Fig. 19), it can be immediately observed how the computed torsional angle is higher, as expected, for the modified blade than for the original one. Moreover, the trend of bending is the same in all plots confirming that observation. Even if Fig. 19b,d,f,h show bending modal angles instead of displacements, they can be directly related.

By comparing Fig. 19b with 19d, and Fig. 19f with 19h, some difference can be observed. The modal angle values depend on the scaling applied and the specific values are not important. Moreover, the modeling of clamping as rigid in the FEM model introduces a different than the measured boundary condition, which modifies the mode shapes. Finally, fitting applied to experimental results gives a smoother behavior but can also introduce some numerical error. Despite these local problems, a good agreement between the overall trend of the twist and bend angle for the measured and simulated results can be observed.

This observation would confirm some discrepancies between the test and simulations, which were already spotted for the 1st mode (Fig. 11).

For the original blade, the bending was decoupled from twisting which was measured (Fig. 19g) and simulated (Fig. 19e). The introduced coupling is clearly visible in the increased torsional response for the simulated (Fig. 19f) and measured results (Fig. 19h).

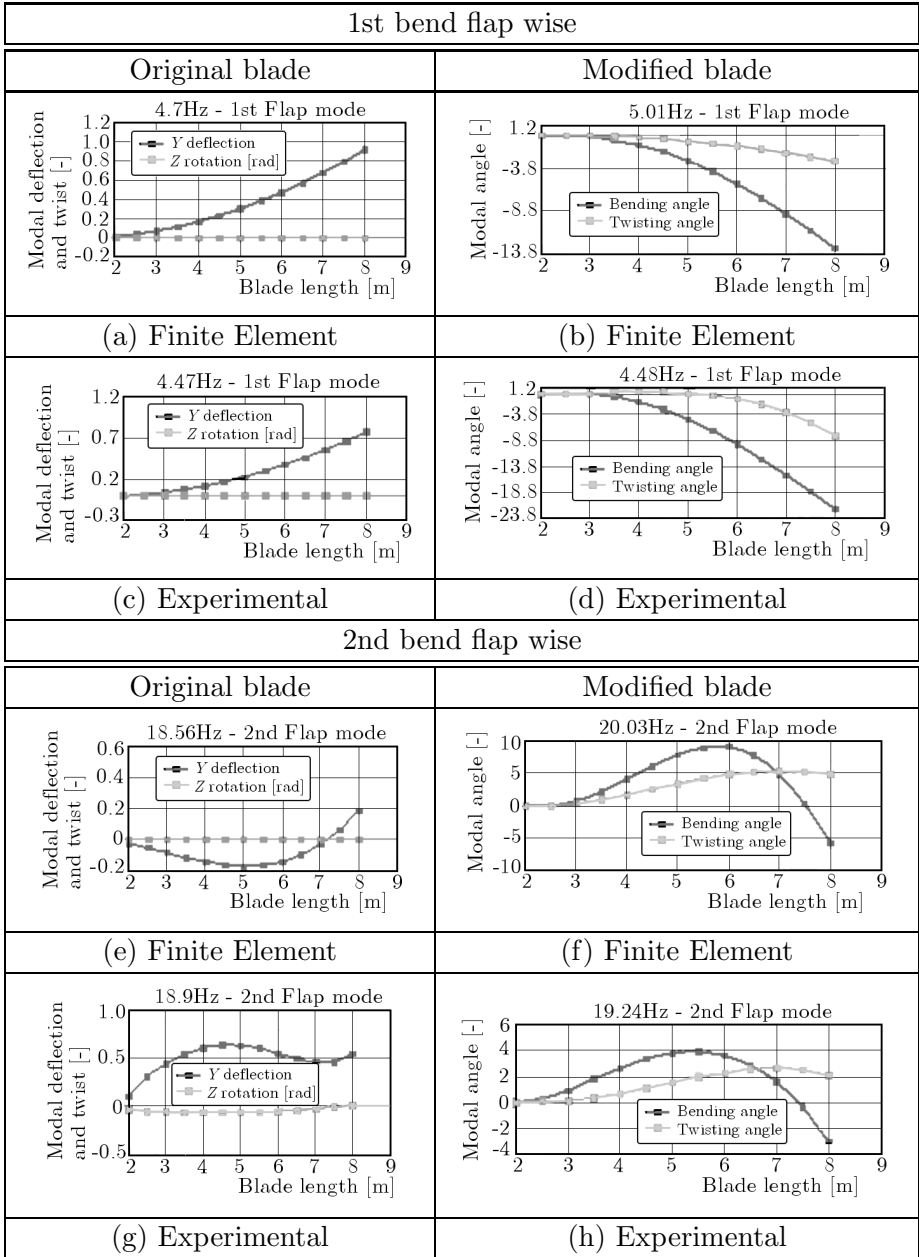


Fig. 19. Twist and bend angle computation from numerical and experimental results for the original (left column) and modified (right column) blade section for 1st and 2nd flapwise bending mode shapes. The blade segment between 2 clamps is not plotted

5.4. Bend-twist coupling index

One of the main objectives is to investigate the amount of twisting introduced by the additional UD layers implemented on the modified blade. To obtain a quantitative measure of the coupling between twisting and bending angle, an index is introduced. For each considered blade cross-section, the ratio between the computed relative twisting and bending angles is evaluated. A coupling index value close to zero means that the twisting is negligible with respect to the bending for the considered mode. On the contrary, a high index value means that twisting is dominant. If the index is close to one, twisting and bending are of the same order of magnitude. Figure 20 shows the computed coupling index for the 1st and 2nd flapwise modes both for the experimental and numerical results.

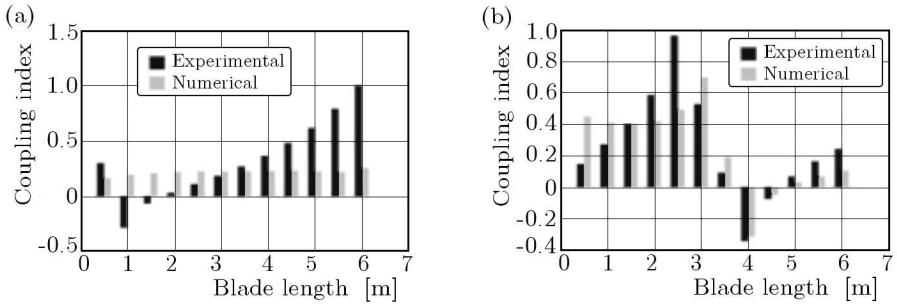


Fig. 20. Bend-twist coupling index for 1st (a) and 2nd (b) flapwise mode

5.5. Discussion of results, problems and proposed improvements

Comparing the numerical and experimental results, certain differences can be observed. These differences are directly related to the observation made for Fig. 11. For the first mode shape, the MAC value between the experiment and numerical model is 65.5. The explanation of the lower MAC value for the 1st mode can be found in the coherence plot presented in Fig. 7. It is a ratio of the maximum energy in a combined output signal due to its various components, and the total amount of energy in the output signal. The coherence is used as a measure of the power in the output channel that is caused by the power in the input or a reference channel. As such, it is useful in assessing the accuracy of the frequency response function measurements. The coherence function can take values that range between 0 and 1. A high value (near 1) indicates that the output is due almost entirely to the input and one can feel confident in the frequency response function measurements. A low value (near 0) indi-

cates problems such as extraneous input signals not being measured, noise, nonlinearities or time delays in the system. The first mode is located in the frequency range of relatively poor coherence leading to the decreased quality of its estimation. The shakers which were used in the measurement have a low frequency limit around 2 Hz. The excitation signal was random that provides homogenous distribution of injected energy over the excited bandwidth. This could lead to the insufficient energy exciting the 1st mode. Moreover, the shakers were hung from support cables. In such a case, at a very low frequency in the sub-10 Hz range there is a problem to provide more inertia to push against the structure being excited for improved performance. To improve the excitation of the 1st mode shape, an additional mass was applied to increase the inertia of the shakers apparently bringing not much improvement. For the 2nd mode located in the higher frequency range of the investigated bandwidth, the vibration amplitudes become lower and the consistency between the test and simulation is much better confirmed by the MAC value of 88.5.

Bend and twist angles calculations are based on the experimental and numerical modal vectors. The difference between the experimental and numerical models bend-twist indexes is caused by the relatively weak excitation of the 1st mode due to the above mentioned reasons.

The supporting structure FEM model should be furthermore updated. The comparison of deformation in the simulated model and the test model shows that the real structure is more flexible. This situation can be caused by uncertainties related to unknown properties of the beam mountings (Fig. 18a), the fact that the beams are drilled (Fig. 18b), the use of I shape clamp beams, while in the real clamp the beams consist of two bolted UPNs (Fig. 18c), and the assumed properties values of plywood, unknown properties of the frame-to-ground mounting.

Further research should introduce two clamps in the FEM model in order to get realistic structural behavior of the clamps. In detail, the plywood plates and steel profiles should be included and contact elements should be applied to model the contact between the clamps and the blade section. It is expected that a more sophisticated support structure FEM representation will improve the consistency between the test and simulations.

The coupling index for the numerical 1st flapwise bending has approximately a constant value throughout the blade, while different behavior is observed from the experiments. In addition to some odd behavior from local mode shapes which could influence the results, it should also be noted that the measured boundary conditions are different than those modeled.

The latter observation can be applied also for the 2nd flap wise bending mode, which on the other hand shows a very similar trend between the numerical and experimental results.

To be able to improve the correlation between the presented results, the same boundary conditions must be used both for the experimental and numerical models.

6. Conclusions

This paper presents some results and aspects of multidisciplinary and interdisciplinary research oriented towards the experimental and numerical study in static and dynamic domains of the bend-twist coupling in the full scale section of a wind turbine blade structure.

An extensive test campaign performed on the original and modified wind turbine blade section was presented. The test setups included different load configurations, excitation and measurement techniques of the contact and non-contact type. Experimental test data examples were shown and used for two purposes. Firstly, to evaluate the ability of different test methods to measure the bend-twist coupling and, secondly, to use the test results for FEM models updating. The common observation from displayed comparisons is that the original blade section did not have a measurable bend-twist coupling. Because one of the primary aims of this work is to develop and use a FEM-model capable of modeling correctly the bend-twist coupling behavior, the original blade section was modified. For this purpose, four UD layers were laminated on the pressure and suction side of the blade section to introduce a measurable flapwise bend-twist coupling.

The successful implementation of the bend-twist coupling was confirmed by extensive static and dynamic measurement campaigns. In both experimental methods, the comparison of original and modified blade properties clearly show the presence of the bend-twist coupling.

Acknowledgements

Vestas Wind Systems A/S has provided and modified the blade sections presented in this study. The work is partly supported by the Danish Energy Authority through the 2007 Energy Research Programme (EFP 2007). The supported EFP-project is titled "Anisotropic beam model for analysis and design of passive controlled wind turbine blades" and has journal no. 33033-0075. The support is gratefully acknowledged and highly appreciated. Authors would like to acknowledge the assistance of Mr.

Philipp Haselbach during the dynamic test campaign. Research presented in Section 5 was conducted in the context of the FP7 project PROND Ref No. 239191. Computations were performed on a 50Tflop cluster in TASK Academic Computer Centre in Gdansk, Poland, within the framework of PL-Grid Project.

References

1. BERRING P., BRANNER K., BERGGREEN C., KNUDSEN H.W., 2007, Torsional performance of wind turbine blades – Part 1: Experimental investigation, *International Conference on Composite Materials (ICCM-16)*, Kyoto, Japan
2. BRANNER K., BERRING P., BERGGREEN C., KNUDSEN H.W., 2007, Torsional performance of wind turbine blades – Part II: Numerical validation, *International Conference on Composite Materials (ICCM-16)*, Kyoto, Japan
3. CAPELLARO M., 2006, *Modeling Bend Twist Coupled Blades*, MSc Thesis, Technical University of Denmark
4. DEILMANN C., 2009, *Passive Aeroelastic Tailoring of Wind Turbine Blades – a Numerical Analysis*, MsC Thesis Thesis (S.M.) – Massachusetts Institute of Technology, Dept. of Mechanical Engineering
5. FEDOROV V.A., DIMITROV N., BERGGREEN C., KRENK S., BRANNER K., BERRING P., 2010, Investigation of structural behaviour due to bend-twist couplings in wind turbine blades, *NAFEMS Nordic Seminar of Simulating Composite Materials and Structures*, Esbjerg, Denmark
6. GRIFFITH D.T., SMITH G., CASIAS M., REESE S., SIMMERMACHER T.W., 2006, *Modal Testing of the TX-100 Wind Turbine Blade*, Sandia Report SAND2005-6454
7. LARSEN G.C., HANSEN M.H., BAUMGART A., CARLÉN I., 2002, *Modal Analysis of Wind Turbine Blades*, Risø-R-1181, Risø National Laboratory, Roskilde, Denmark
8. LOBITZ D.W., LAINO D.J., 1998, Load mitigation with twist-coupled HAWT blades, *Proceedings of 1998 ASME Wind Energy Symposium*, January
9. LOBITZ D.W., VEERS P.S., 1999, Aeroelastic behavior of twist-coupled HAWT blades, *Proceedings of 1999 ASME Wind Energy Symposium*, January
10. LOBITZ D.W., VEERS P.S., EISLER G.R., LAINO D.J., MIGLIORE P.G., BIR G., 2001, *The Use of Twisted-Coupled Blades to Enhance the Performance of Horizontal Axis Wind Turbines*, Sandia Report SAND01-1303

11. LOCKE J., HILDAGO I.C., 2002, *The Implementation of Braided Composite Materials in the Design of a Bend-Twist Coupled Blade*, Sandia Report SAND02-2425
12. LOCKE J., VALENCIA U., 2004, *Design Studies for Twisted-Coupled Wind Turbine Blades*, Sandia Report, SAND04-0522
13. LUCZAK M., BRANNER K., BERRING P., MANZATO S., HASELBACH P., PEETERS B., 2011, Experimental verification of the implementation of bend-twist coupling in a wind turbine blade, [In:] *Scientific Proceedings of EWEA2011 European Wind Energy Conference 2011*, Brussels, Belgium
14. LUCZAK M., DZIEDZIECH K., VIVOLO M., DESMET W., PEETERS B., VAN DER AUWERAER H., 2010, Contact versus non-contact measurement of a helicopter main rotor composite blade, *9th International Conference on Vibration Measurements By Laser and Noncontact Techniques, AIVELA 2010*, Ancona, Italy
15. ONG C.-H., TSAI S.W., 1999, *Design, Manufacture and Testing of a Bend-Twist D-spar*, Sandia Report SAND99-1324
16. PEDERSEN H.B, KRISTENSEN O.J.D., 2003, *Applied Modal Analysis of Wind Turbine Blades*, Risø-R-1388(EN), Risø National Laboratory, Roskilde, Denmark
17. PEETERS B., VAN DER AUWERAER H., GUILLAUME P., LEURIDAN J., 2004, The polymax frequency-domain method: a new standard for modal parameter estimation? *Shock And Vibration, Special Issue dedicated to Professor Bruno Piombo*, **11**, 395-409
18. WALSH J.M., 2009, *Composite Material Bend-Twist Coupling for Wind Turbine Blade Applications*, MsC Thesis, University of Wyoming, Department of Mechanical Engineering
19. ZUTECK M., 2002, *Adaptive Blade Concept Assessment: Curved Planform Induced Twist Investigation*, Sandia Report SAND02-2996

Badania eksperymentalne i symulacyjne sprzężenia typu zginanie-skręcanie w dynamice łopaty turbiny wiatrowej

Streszczenie

W artykule przedstawiono wyniki multidyscyplinarnych prac badawczych prowadzonych na sekcji dużej łopaty turbiny wiatrowej. Prace obejmowały badania eksperymentalne oraz symulacje numeryczne sprzężenia typu zginanie-skręcanie w statyce i dynamice badanej łopaty. Podstawowym celem badawczym było potwierdzenie

w drodze eksperymentu wyników symulacji numerycznej własności statycznych i dynamicznych łopaty.

Sprzężenie typu zginanie-skręcanie zostało wprowadzone w konstrukcji łopaty poprzez dodatkowe zalaminowanie warstw kompozytów włóknistych jednokierunkowych po obu stronach łopaty pod dobranym kątem. Testy statyczne i dynamiczne zostały zrealizowane na sekcji dużej łopaty turbiny wiatrowej dostarczonej przez producenta Vestas Wind Systems A/S. W pracy przedstawiono i porównano wyniki badań oryginalnej sekcji łopaty oraz sekcji zmodyfikowanej. Analiza porównawcza wyników potwierdziła wyniki symulacji numerycznych. Wprowadzenie dodatkowych warstw kompozytu włóknistego spowodowało powstanie w badanej łopacie mierzalnego sprzężenia typu zginanie-skręcanie. Sprzężenie to nie było obserwowane w oryginalnej łopacie przed modyfikacją.

Manuscript received March 7, 2011; accepted for print May 19, 2011